AN IN-VITRO EXPERIMENTAL SETUP FOR FLOW CHARACTERIZATION ON PROLAPSED AND PERFORATED MITRAL VALVE MODELS

R. P. Jong^{1,2*}, M.I. Kori³, K. Osman¹, M. N. A. W. M. Yazid¹, , A. B. N. I. Rosli³ and A.Z.M. Khudzari³

¹Faculty of Mechanical Engineering.
Universiti Teknologi Malaysia, Johor Bahru, 81310, Johor, Malaysia.

²Department of Mechanical and Manufacturing Engineering,
Faculty of Engineering.
Universiti Malaysia Sarawak, Kota Samarahan, 94300, Sarawak, Malaysia.

³Department of Biomedical Engineering & Health Science,
Faculty of Electrical Engineering.
Universiti Malaysia Sarawak, Kota Samarahan, 94300, Sarawak, Malaysia.

*Corresponding Author's Email: 1jprudiyanto@unimas.my

Article History: Received Oct 08, 2025; Revised Nov 04, 2025; Accepted Nov 06, 2025

ABSTRACT: The mitral valve is one of the important parts of the heart valve that prevents blood from regurgitating into the left atrium. Mitral regurgitation is the most common cause of regurgitation, affecting approximately 176 million people worldwide and 2-3% of the general population. Flow dynamics parameters are important for evaluating regurgitation severity, which can be done through flow simulation. However, there are limited open-access datasets available for validating the simulated output. This paper presented an experimental setup that can serve as a validation tool for flow simulation output. The in-vitro setup was tested by evaluating flow behaviour through a defective mitral heart valve. The results show consistent readings validated against published data. The correlation between flow rate and the pressure difference between the left ventricle and the left atrium follows the principles of fluid dynamics for flow through an orifice. Hence, this in vitro setup can be used as a validation tool for flow simulation results, especially for heart valves.

KEYWORDS: In-vitro Hemodynamics Analysis; Mitral Valve Perforation; Flow Evaluation Apparatus

1.0 INTRODUCTION

Mitral valve prolapse (MVP) is the leading cause of mitral regurgitation, affecting about 176 million people globally and 2-3% of the general population [1]. Mitral valve prolapse (MVP) is the most common etiology of primary mitral regurgitation (MR), defined as regurgitation caused by a structural abnormality or defect of the mitral valve leaflets [2]. The systolic movement of portions or segments of the mitral leaflets into the left atrium is characteristic of MVP. Severe MR typically results from anatomical disruptions such as a flail leaflet (the free edge moving into the left atrium) [3], often caused by chordal rupture, and most likely to cause severe MR [4]. Dynamic variations frequently characterize mitral regurgitation caused by MVP, and in some patients, the regurgitation may be temporally limited to mid- or late systole, complicating its overall assessment. Mitral perforation (MP) is recognized as a rare but significant cause of severe MR [5, 6]. The physical characteristics of the perforation directly influence the regurgitant flow pattern and severity. Even a tiny perforation can produce an MR jet that is sufficient to cause severe complications to the atrial wall [7]. Given that MR resulting from perforation often leads to severe MR, surgical intervention for repair or replacement of the mitral valve is usually recommended as soon as possible. Flow dynamics parameters are essential for assessing MR severity [8]. The gold standard for evaluating mitral regurgitation by echocardiogram [9] defines regurgitation severity based on effective regurgitant orifice area (EROA), regurgitant volume (RVol), and regurgitant fraction (RF) [10]. The most commonly employed flow-based technique is the flow convergence method, also known as the proximal isovelocity surface area (PISA) method [11], which allows both qualitative assessment and calculation of the instantaneous peak flow rate. Additionally, the vena contracta (VC) width, which represents the path of the regurgitant jet, is measured using flow techniques. MR is often dynamic, meaning that the EROA and flow rate fluctuate throughout systole, particularly in

primary MR. In such cases (e.g., late systolic MR), the flow-derived regurgitant volume is often a more reliable index of severity than a single EROA measurement, which might overestimate the true extent of regurgitation [12]. Validation of computationally simulated mitral flow is typically performed using medical imaging data such as echocardiography, computed tomography (CT), or magnetic resonance imaging (MRI) [13]. However, the use of such medical data requires prior ethical approval [14,15], and open-access datasets remain limited [16–18]. These constraints reduce the feasibility of reliable model validation using real patient data.

Therefore, this study aims to design and evaluate an in vitro experimental setup to analyze the flow behaviour of mitral regurgitation caused by valve prolapse and perforation under steady-state conditions. The proposed setup is intended to serve as a validation and reference tool for computational fluid dynamics (CFD) simulations, assisting in defining the initial setup and boundary conditions and verifying the accuracy of simulated outputs.

2.0 METHODOLOGY

The study involves implementing an in vitro experimental setup for hemodynamic analysis, with a specific focus on assessing flow behaviour through a defective mitral heart valve. The objective is to examine the flow characteristics associated with mitral valve prolapse, which can lead to mitral regurgitation.

2.1 Experimental Rig Setup

The experimental rig presented in this paper was a low-cost, simplified version of the Ott et al. setup [19]. The main components of the experimental rig include a flow chamber, a pump, a fluid reservoir, and piping serving as the liquid flow channel. The measurement components were pressure transducers and a flow meter. Figure 1 shows the schematic diagram of the experimental rig setup used in the current study.

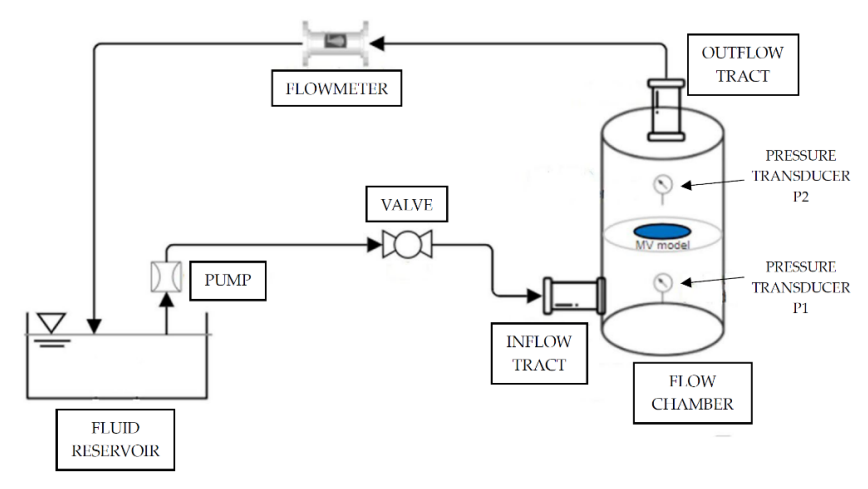


Figure 1: Schematic diagram of experimental rig setup

Figure 2 shows the overall experimental rig setup. Water is used as the fluid for the experimental setup in this study. Fluid is pumped from the fluid reservoir and controlled by the flow control valve into the flow chamber, as shown by the flow direction arrows. The fluid exits the flow chamber and returns to the fluid reservoir, forming a closed circuit throughout the experiment.

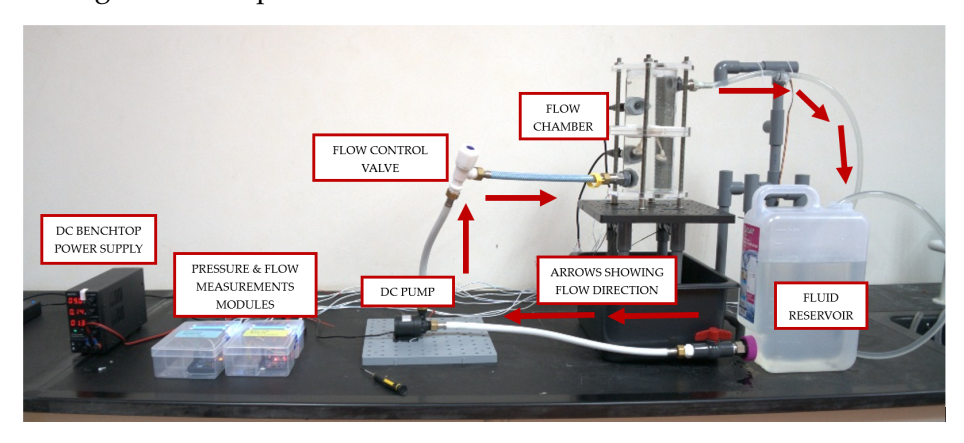


Figure 2: Overall experimental rig setup

Pump control with a DC voltage regulator to control pump speed, thereby directly controlling the fluid flow. Additionally, the flow control valve regulated the system's flow. Pressure differences were measured with pressure transducers mounted on the flow chamber.

The system flow rate was measured with a flowmeter fitted at the exit tube after the exit tract of the flow chamber. The flow chamber design is shown in Figure 3. The flow chamber consists of two sections representing the left atrium and the left ventricle in this study. The flow direction upward represents the flow towards the left atrium from the left ventricle during the closure of the mitral valve apparatus. The build dimensions of the flow chamber are summarized in Table 1.

Each chamber section was fitted with low-cost pressure transducers to measure the pressure difference, P1 – P2. In this setup, P1 represents the pressure in the left ventricle, and P2 represents the pressure in the left atrium. The pressure transducers can measure up to 10 psi. A flow meter was installed after the outflow tract, using the principle of flow continuity: at any point along the flow path, the flow rate is constant. Both pressure transducers and a flow meter were connected to a separate Arduino module for direct readings. The flow meter module directly measures the flow rate, while the pressure measurement module measures the difference between the pressure transducers P1 and P2 (P1 – P2). The flow and pressure measurement modules are shown in Figure 4.

Table 1: Summary of parameters for the flow chamber

Chamber diameter	0.1016 m
Chamber height	0.3302 m
Flow channel cross-sectional area	0.0081 m ²
Inlet and outlet tract diameter	15 mm

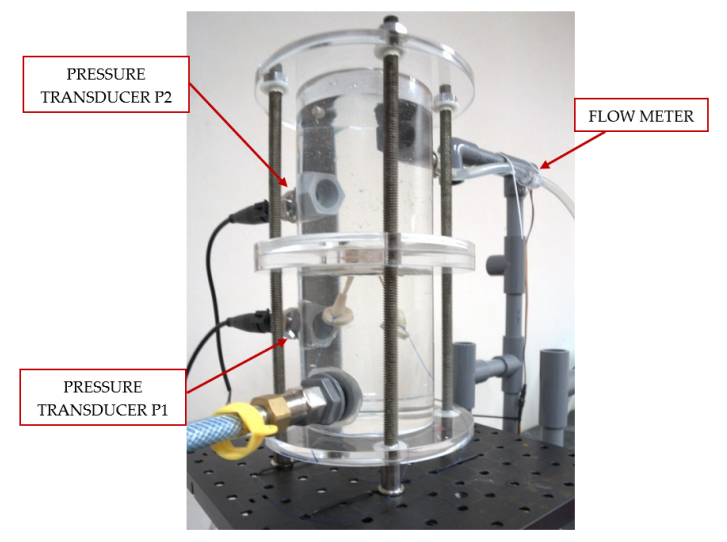


Figure 3: Flow chamber setup

Flow evaluation was performed by controlling the fluid flow rate through the system based on flow meter readings. The flow was controlled by variation of valve opening after the pump or by varying the voltage supplied to the pump. Pressure difference of P1-P2 was recorded with respect to each flow rate reading of the flow measurement module.

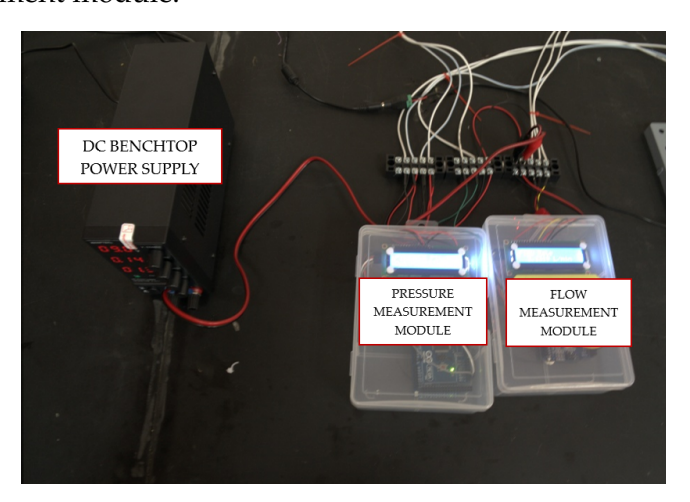


Figure 4: Pressure and flow measurements modules

2.2 Mitral Valve Apparatus

The mitral valve apparatus used in the study, as shown in Figure 5, was the LifeLike Biotissue Mitral Valve Model [20]. The model was a prolapsed mitral valve at the posterior leaflet, making it a good model for evaluating mitral regurgitation due to mitral valve prolapse.

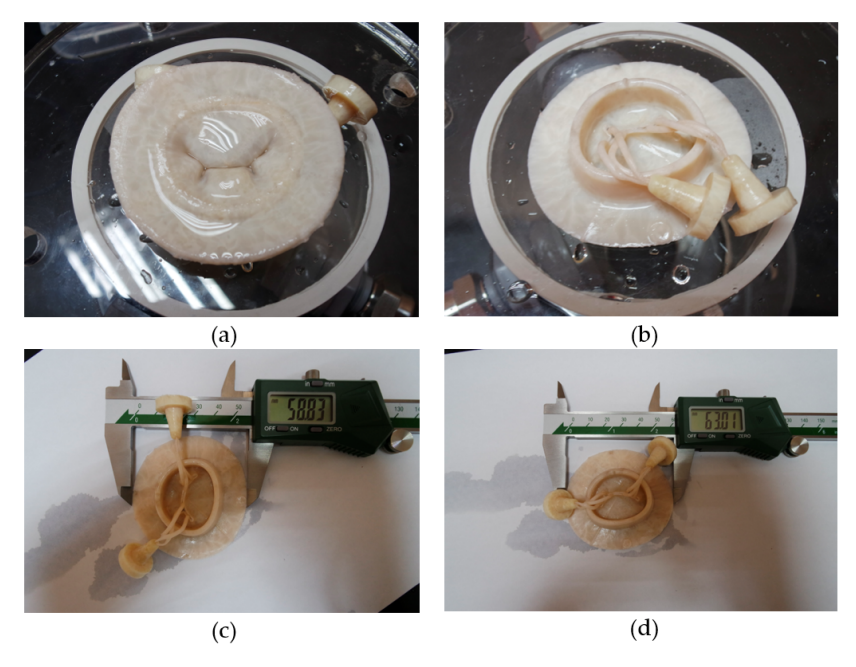


Figure 5: Mitral valve apparatus; (a) top view, (b) bottom view, (c) width measurement, (d) length measurement

A mitral valve apparatus with perforation was created based on three conditions: mild, moderate, and severe [21]. Mild perforation is created with a 3.5 mm diameter hole on the anterior leaflet. At the same time, 5.0 mm and 7.0 mm perforation diameters represent moderate and severe perforations, respectively. The perforation sample on the mitral valve leaflet is shown in Figure 6.

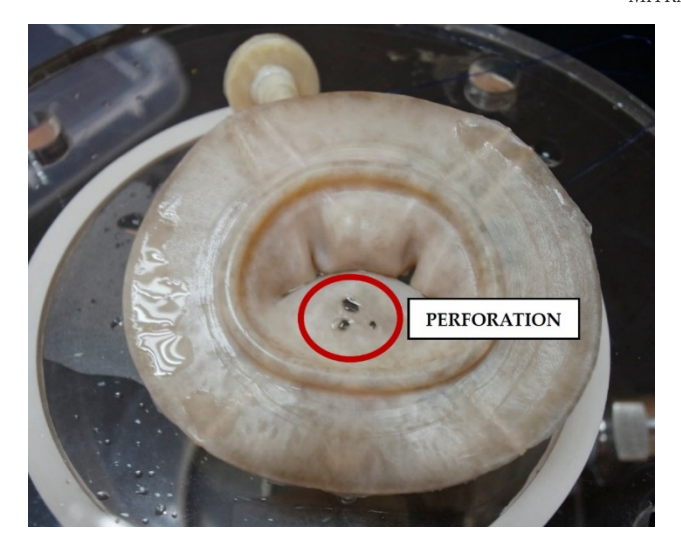


Figure 6: Mitral valve apparatus with 7.0 mm perforation

2.3 Calibrations

During the calibration of the flow sensor, a 1-litre beaker was used as the reference vessel, and a timer was used to measure the time required for the fluid to fill it. A series of 10 flow rate readings was taken digitally and manually under identical conditions.

These manually calculated flow rate values were then compared with the experimental readings obtained directly from the flow meter display. Any differences between the actual and experimental values are accounted for by adjusting the sensor's calibration factor (K), which was obtained from the sensor's datasheet (previously noted as K = 22000 pulses per litre).

For the pressure transducer calibration, which operates with an input range of 0-5V and measures pressures up to 10 psi, analog readings are converted to voltage values to determine pressure. An analog reading (AnalogRead) is mapped to voltages from 0.5V to 5V, corresponding to values from 0 to 1023 in the ADC (Analog-to-Digital Converter), where *X* is an analog reading and 1024 is the maximum value for a 10-bit ADC.

The pressure values at zero and at maximum are determined using Equations 2.1 and 2.2, respectively:

$$\frac{X}{1024} = \frac{0.5 \text{ V}}{5 \text{ V}} (zero \, pressure) \tag{2.1}$$

$$\frac{X}{1024} = \frac{4.5 \text{ V}}{5 \text{ V}} (maximum \, pressure) \tag{2.2}$$

These equations define how *X*, representing pressure, is calculated from voltage inputs of 0.5V and 4.5V, corresponding to zero and maximum pressure, respectively, within a 5V range.

3.0 RESULTS

3.1 Results validation

The average values of the measurements in the current study are compared with those reported by Ott et al. [19], as shown in Figure 7. The results of the current study closely correlated with Ott's. Hence, indicating that the setup is acceptable for the next steps of the experiments. Ott recorded only parameters with a flow rate of less than 0.6 l/min and a pressure difference of less than 120 mmHg. At the same time, the current study extended the readings to an average flow rate of 1.2 l/min and a pressure difference of 153 mmHg. The extension of the measurement represents a further degree of mitral regurgitation severity not covered by the previous study.

Experiment readings were repeated three times for each case of the mitral valve apparatus, with and without perforation. All readings showed a near-quadratic correlation. Average readings of all three measurements are shown in Figure 7, along with a comparison to Ott's results. Figure 8 illustrates the haemodynamic performance of the prolapse mitral valve model (without perforation), measured three times with a similar setup. In the low-flow region below 0.5 l/min, all measurements are tightly clustered, indicating excellent repeatability of the experimental system and the

low-flow region. The data begin to scatter above 0.6 l/min. The measurements continued up to about 1.2 l/min, with a pressure difference of about 130-160 mmHg.

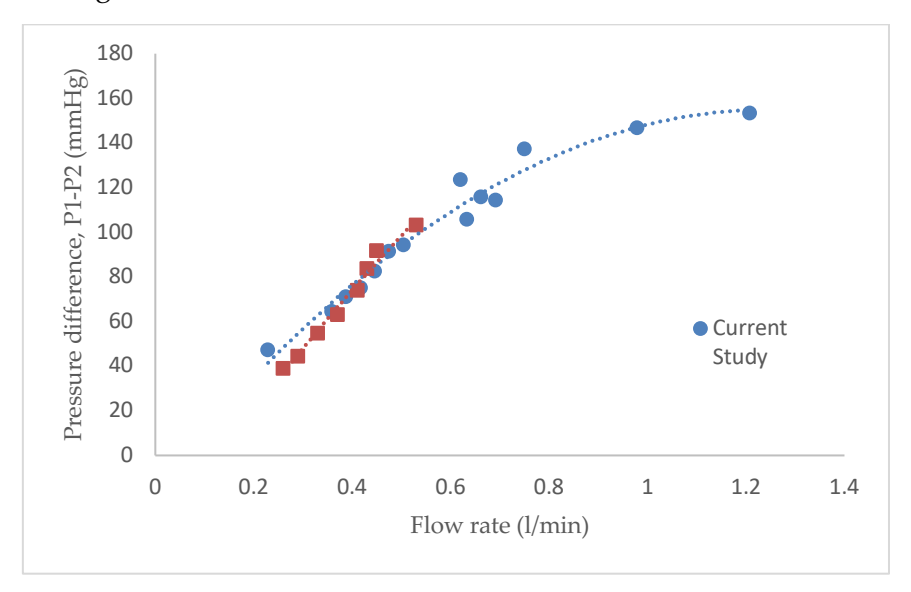


Figure 7: Comparison between the results from this study and Ott's results

Although there are differences in the recorded pressure differences with respect to flow rate among the three measurements, the correlations for all measurements are consistent. All three measurements showed quadratic correlations with the general form given in Equation 2.3.

$$\Delta P = aQ^2 + bQ + c \tag{3.3}$$

where, ΔP is the pressure difference (P1-P2), Q is the flow rate. The coefficients of a, b, and c are shown in Table 2.

Table 2: Quadratic correlation coefficients for prolapse mitral valve without perforation

Measurements	а	b	С
Measurement 1	-109.79	272.99	-24.20
Measurement 2	-104.03	275.26	-12.36
Measurement 3	-140.28	315.27	-27.02

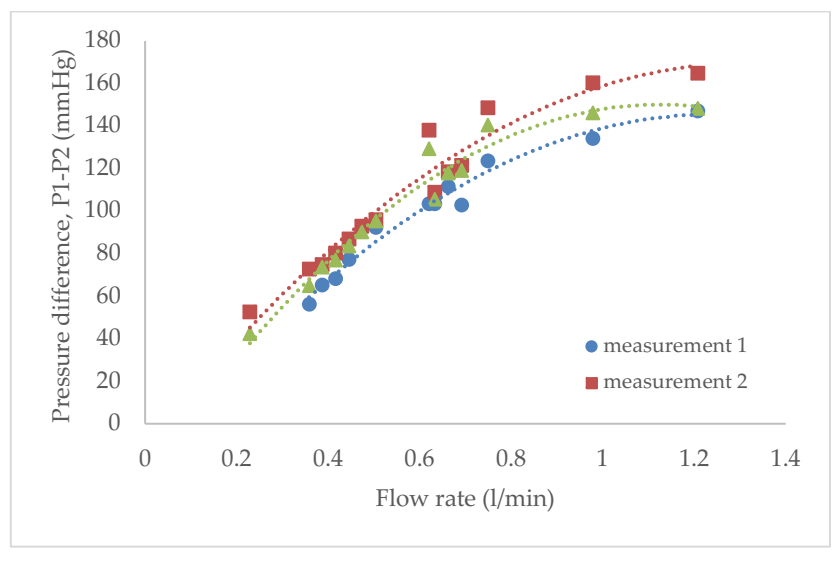


Figure 8: Measurements of pressure difference against flow rate through the prolapse mitral valve apparatus

Average measurements of pressure difference between the left atrium and left ventricle for the perforated mitral valve apparatus are shown in Figure 9. Three perforation sizes representing the average severity of mitral valve perforations were evaluated: 3.5 mm (mild), 5.0 mm (moderate), and 7.0 mm (severe).

In the mitral valve with all perforation diameters recorded, lower pressure differences were observed in transmitral flow rate compared with the mitral valve apparatus without perforations. Mitral valve apparatus with a 3.5 mm perforation diameter recorded a pressure difference of 31 mmHg at the lowest flow rate. In comparison, perforation sizes of 5.0 mm and 7.0 mm resulted in 14 mmHg and 17 mmHg, respectively. The pressure difference dropped by almost half with increased perforation sizes of 1.5 mm and 3.5 mm in the current study. The valve without perforation recorded a pressure difference of 48 mmHg, higher than in any perforated valve condition. Similar to the mitral valve without perforation, the mitral valve with perforation also demonstrated close-to-quadratic correlations between pressure difference and flow rate, as in Equation 2.3. The coefficients for the mitral valve without perforation (average readings) and the mitral valve with perforation are recorded in Table 3.

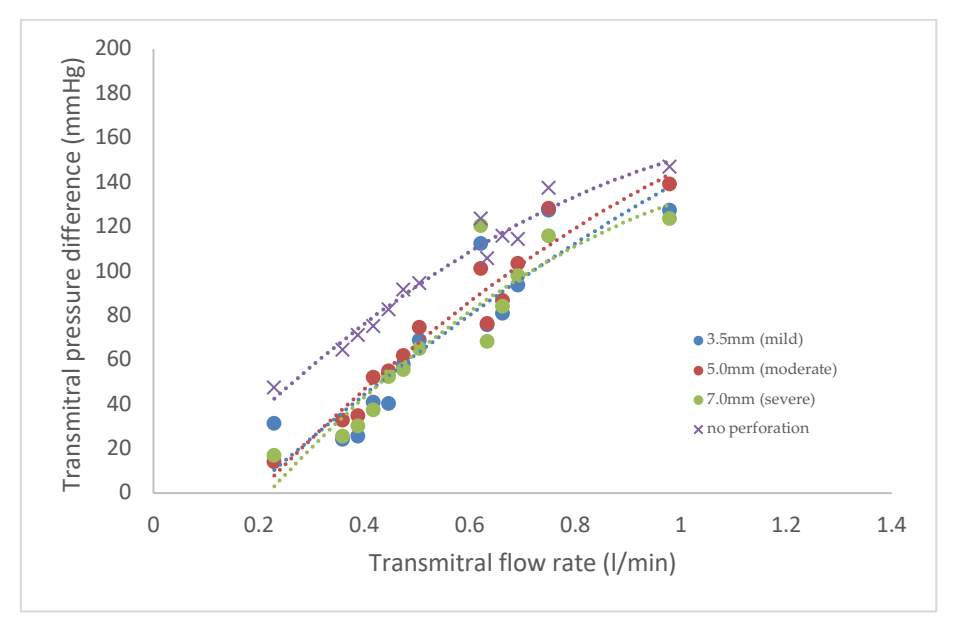


Figure 9: Measurements of pressure difference against flow rate through the perforated mitral valve apparatus

Table 3: Quadratic correlation coefficients for prolapse mitral valve with perforation

Perforation diameter	а	b	С		
3.5 mm (mild)	-48.24	228.42	-39.39		
5.0 mm (moderate)	-79.65	277.11	-51.39		
7.0mm (severe)	-112.92	305.80	-61.08		
No perforation (average)	-94.00	256.37	-11.29		

Figure 10 shows examples of mitral valves with and without perforation, viewed from the top of the flow chamber during the experiments. It can be observed that the openings at the coaptation zones are larger in the mitral valve with perforation than in the mitral valve without perforation. The flow through the perforation has possibly caused lower transmitral pressure and an increase in left atrial pressure, leading to a larger opening at the coaptation zone.



Figure 10: Mitral valve apparatus viewed from the left atrium side during the experiment (a) prolapse valve, (b) prolapse and perforated valve

4.0 DISCUSSIONS

The mitral valve apparatus without perforation presented in this paper exhibited leakage (regurgitation) at increased flow rates, thereby directly increasing ventricular pressure (P1). This situation explained the continuous flow exiting the flow chamber throughout the experimental process. As the pressure in the ventricle, P1, increased, the pressure difference, P1-P2, also increased due to the increased flow rate from the pump, forcing the valve leaflet to leak and increasing regurgitation. The relationship between the volumetric flow rate and the resulting pressure difference is critical to determine the hemodynamic burden of mitral regurgitation. This study characterized this relationship experimentally, with the averaged results presented in Figure 7. As the regurgitant flow rate increases, the blood flow becomes increasingly turbulent [22], leading to greater energy dissipation and a larger pressure difference across the prolapsed valve. To validate the physiological accuracy of our model, these findings were benchmarked against published data by Ott et al., which showed strong agreement in the low-flow region.

The experiment was repeated three times under identical conditions, as detailed in Figure 8, to test the reliability of the results. The high degree of consistency, especially in the low-flow region, confirms that the resulting correlations are not due to random error. Therefore, the consistency shown in Figure 8 reinforces the key finding: as mitral

regurgitation worsens, the pressure load on the left atrium rises in a polynomial relationship with the flow rate. This statement provides a clear fluid-dynamic basis for understanding the progressive left atrial dilation and other clinical symptoms in patients with this condition. The presence of a perforation, as shown in Figure 9, leads to a significantly lower transmitral pressure difference. This phenomenon may be due to fluid dynamics, in which the perforation provides an additional, less restrictive pathway for regurgitant flow, effectively increasing the total effective orifice area. This larger orifice offers less resistance, thereby reducing the pressure gradient required to induce the same volume of flow as compared to the mitral valve without perforation [23].

The clinical implications of these findings are significant. As shown in Figure 9, the magnitude of the pressure difference is inversely related to the size of the perforation; a larger, more severe defect results in a lower pressure gradient. This result suggests that in a clinical setting, relying solely on Doppler-derived pressure gradients could be misleading for assessing the severity of regurgitation caused by leaflet perforation [24, 25]. Therefore, this study highlights that the hemodynamic indication of perforation-induced regurgitation is fundamentally different from that of pure leaflet prolapse. However, simulation studies still require robust validation tools for their results, and the setup proposed in this study is a reliable tool for that purpose.

Limitations of the current study were on the fluid type, flow range, and the flow type:

- i. Water was used in this study, which might not reflect the actual properties of blood.
- ii. The low flow range was evaluated based on the limitations of water flow through the mitral valve.
- iii. The flow involved was steady-state, which might not represent the actual regurgitation flow behaviour.

5.0 CONCLUSIONS

This paper presents an evaluation of the hemodynamics of the mitral valve apparatus using a flow chamber. The perforated mitral valve apparatus showed a lower pressure difference than the non-perforated mitral valve apparatus at a similar flow rate. The developed in vitro rig demonstrated consistent, reproducible flow-pressure relationships that closely matched published data, confirming its reliability as a platform for experimental validation of computational hemodynamic simulations of mitral valve flow.

CONFLICT OF INTEREST STATEMENT

The authors have no conflicts of interest to declare and are in agreement with the contents of the manuscript.

ACKNOWLEDGMENTS

The authors would like to acknowledge financial support from Universiti Teknologi Malaysia through the UTM Encouragement Research Grant (UTMER) (Q.J130000.3823.31J13).

6.0 REFERENCES

- [1] P. Patel, K. Lee, A. Aderinto, M. Benz, and A. Tsompanidis, "Assessment and management of a 1.77-cm(2) mitral leaflet perforation as a subclinical cause of mitral regurgitation," (in eng), *Clin Case Rep*, vol. 6, no. 10, pp. 1961-1965, Oct 2018.
- [2] E. Apostolidou, A. D. Maslow, and A. Poppas, "Primary mitral valve regurgitation: Update and review," (in eng), *Glob Cardiol Sci Pract*, vol. 2017, no. 1, p. e201703, Mar 31 2017.
- [3] A. P.-W. Lee *et al.*, "Quantitative Analysis of Mitral Valve Morphology in Mitral Valve Prolapse With Real-Time 3-Dimensional Echocardiography," vol. 127, no. 7, pp. 832-841, 2013.
- [4] C. Antoine *et al.*, "Pathophysiology of Degenerative Mitral Regurgitation," vol. 11, no. 1, p. e005971, 2018.
- [5] A. S. Gurbuz *et al.*, "Perforation of anterior mitral leaflet aneurysm: A rare cause of severe mitral regurgitation," *The Egyptian Heart Journal*,

- vol. 68, no. 2, pp. 131-133, 2016/06/01/2016.
- [6] T. Yamanaka, M. Higashitani, Y. Ichinohe, T. Fukatsu, and T. Kunihara, "Infective endocarditis with perforation of the anterior mitral valve leaflet due to mild aortic regurgitation: a case report," (in eng), *Eur Heart J Case Rep*, vol. 9, no. 3, p. ytaf076, Mar 2025.
- [7] A. Naito *et al.*, "Severe haemolytic anaemia and acute renal failure caused by pinhole perforation of native mitral valve: a case report," (in eng), *Eur Heart J Case Rep*, vol. 9, no. 7, p. ytaf290, Jul 2025.
- [8] C. M. Otto et al., "2020 ACC/AHA Guideline for the Management of Patients With Valvular Heart Disease: Executive Summary: A Report of the American College of Cardiology/American Heart Association Joint Committee on Clinical Practice Guidelines," vol. 143, no. 5, pp. e35-e71, 2021.
- [9] A. Hagendorff *et al.*, "Echocardiographic assessment of mitral regurgitation: discussion of practical and methodologic aspects of severity quantification to improve diagnostic conclusiveness," (in eng), *Clin Res Cardiol*, vol. 110, no. 11, pp. 1704-1733, Nov 2021.
- [10] P. G. Chew, K. Bounford, S. Plein, D. Schlosshan, and J. P. Greenwood, "Multimodality imaging for the quantitative assessment of mitral regurgitation," (in eng), *Quant Imaging Med Surg*, vol. 8, no. 3, pp. 342-359, Apr 2018.
- [11] R. Leister *et al.*, "Investigating the Shortcomings of the Flow Convergence Method for Quantification of Mitral Regurgitation in a Pulsatile In-Vitro Environment and with Computational Fluid Dynamics," (in eng), *Cardiovasc Eng Technol*, vol. 16, no. 2, pp. 155-170, Apr 2025.
- [12] D. M. Toader, "Echocardiographic quantification of mitral apparatus morphology and dynamics in patients with dilated cardiomyopathy," (in eng), *J Int Med Res*, vol. 52, no. 2, p. 3000605231209830, Feb 2024.
- [13] M. Hedayat, T. R. Patel, T. Kim, M. Belohlavek, K. R. Hoffmann, and I. Borazjani, "A hybrid echocardiography-CFD framework for ventricular flow simulations," (in English), *International Journal for Numerical Methods in Biomedical Engineering*, Article vol. 36, no. 7, p. 22, Jul 2020, Art. no. e03352.
- [14] I. Hackett and R. P. Ward, "Appropriate Use Criteria for Echocardiography in the Era of Value-Based Care: Mission Accomplished or Future Mandates?," (in eng), *Curr Cardiol Rep*, vol. 22, no. 8, p. 69, Jun 19 2020.
- [15] S. T. Padmapriya and S. Parthasarathy, "Ethical Data Collection for Medical Image Analysis: a Structured Approach," (in eng), *Asian Bioeth*

- Rev, vol. 16, no. 1, pp. 1-14, Apr 10 2023.
- [16] M. Nievas Offidani, F. Roffet, M. C. González Galtier, M. Massiris, and C. Delrieux, "An Open-Source Clinical Case Dataset for Medical Image Classification and Multimodal AI Applications," vol. 10, no. 8, p. 123, 2025.
- [17] Z. Liu, Q. Lv, C. H. Lee, and L. Shen, "Segmenting medical images with limited data," *Neural Networks*, vol. 177, p. 106367, 2024/09/01/2024.
- [18] A. Alabduljabbar, S. U. Khan, A. Alsuhaibani, F. Almarshad, and Y. N. Altherwy, "Medical imaging datasets, preparation, and availability for artificial intelligence in medical imaging," vol. 8, no. 1, pp. 1471-1483, 2024.
- [19] R. Ott *et al.*, "Development of an experimental setup for the in vitro investigation of mitral valve repair devices," *Current Directions in Biomedical Engineering*, vol. 5, no. 1, pp. 501-503, 2019.
- [20] LifeLike BioTissue. (2025, 25 September). *Mitral Valve Model*. Available: https://lifelikebiotissue.com/shop/cardiac/mitral-valv
- [21] J. Brenneisen, C. Wentzel, F. Karwan, O. Dössel, and A. Loewe, "Fluid dynamics in the human heart: Altered vortex formation and wash-out in mitral regurgitation simulations," vol. 7, no. 2, pp. 199-202, 2021.
- [22] K. M. Saqr *et al.*, "Physiologic blood flow is turbulent," *Scientific Reports*, vol. 10, no. 1, p. 15492, 2020/09/23 2020.
- [23] A. Golijanek-Jędrzejczyk and A. Mrowiec, "Cylindrical orifice testing in laminar flow with the orifice diameter ratio β = 0.5," (in eng), *Sci Rep*, vol. 13, no. 1, p. 15411, Sep 18 2023.
- [24] A. Diwan, M. McCulloch, G. M. Lawrie, M. J. Reardon, and S. F. Nagueh, "Doppler Estimation of Left Ventricular Filling Pressures in Patients With Mitral Valve Disease," vol. 111, no. 24, pp. 3281-3289, 2005.
- [25] B. R. Gebhardt, "Knowing the Limits: Pitfalls of Echocardiography in Mitral Regurgitation," *Journal of Cardiothoracic and Vascular Anesthesia*, vol. 34, no. 1, pp. 294-296, 2020.